



The hydrologic consequences of land cover change in central Argentina

M.D. Nosetto^{a,b,c,*}, E.G. Jobbágy^{a,c}, A.B. Brizuela^{b,d}, R.B. Jackson^{e,f}

^a Grupo de Estudios Ambientales, IMASL, Universidad Nacional de San Luis & CONICET, San Luis, Argentina

^b Cátedra de Climatología Agrícola, Facultad de Ciencias Agropecuarias, Universidad Nacional de Entre Ríos, Argentina

^c Departamento de Agronomía, FICES, Universidad Nacional de San Luis, San Luis, Argentina

^d Centro de Investigaciones Científicas y Transferencia de Tecnología a la Producción, CONICET, Diamante, Entre Ríos, Argentina

^e Department of Biology and Nicholas School of the Environment and Earth Sciences, Duke University, Durham, NC, USA

^f Center on Global Change, Duke University, Durham, NC, USA

ARTICLE INFO

Article history:

Received 28 June 2010

Received in revised form 4 January 2011

Accepted 11 January 2011

Available online 4 February 2011

Keywords:

Land-use change

Water yield

Evapotranspiration

Dry forests

Landsat

ABSTRACT

Vegetation exerts a strong control on water balance and key hydrological variables like evapotranspiration, water yield or even the flooded area may result severely affected by vegetation changes. Particularly, transitions between tree- and herbaceous-dominated covers, which are taking place at increasing rates in South America, may have the greatest impact on the water balance. Based on Landsat imagery analysis, soil sampling and hydrological modeling, we evaluated vapor and liquid ecosystem water fluxes and soil moisture changes in temperate Argentina and provided a useful framework to assess potential hydrological impacts of vegetation cover changes. Two types of native vegetation (grasslands and forests) and three modified covers (eucalyptus plantations, single soybean crop and wheat/soybean rotation) were considered in the analysis. Despite contrasting structural differences, native forests and eucalyptus plantations displayed evapotranspiration values remarkably similar ($\sim 1100 \text{ mm y}^{-1}$) and significantly higher than herbaceous vegetation covers (~ 780 , ~ 670 and $\sim 800 \text{ mm y}^{-1}$ for grasslands, soybean and wheat/soybean (*Triticum aestivum* L., *Glycine max* L.) system, respectively). In agreement with evapotranspiration estimates, soil profiles to a depth of 3 m were significantly drier in woody covers ($0.31 \text{ m}^3 \text{ m}^{-3}$) compared to native grasslands ($0.39 \text{ m}^3 \text{ m}^{-3}$), soybean ($0.38 \text{ m}^3 \text{ m}^{-3}$) and wheat/soybean rotation ($0.35 \text{ m}^3 \text{ m}^{-3}$). Liquid water fluxes (deep drainage + surface runoff) were at least doubled in herbaceous covers, as suggested by modeling ($\sim 170 \text{ mm y}^{-1}$ and $\sim 357 \text{ mm y}^{-1}$, for woody and herbaceous covers, respectively). Our analysis revealed the hydrological outcomes of different vegetation changes trajectories and provided valuable tools that will help to anticipate likely impacts, minimize uncertainties and provide a solid base for sustainable land use planning.

© 2011 Elsevier B.V. All rights reserved.

1. Introduction

Through their influence on water demand and supply, plants exert strong controls over many key hydrologic variables. In consequence, changes in land cover can affect the water balance and the quantity and quality of water resources. Aerodynamic roughness, albedo and leaf area seasonality are examples of key plant variables that affect water demand and shape evapotranspiration patterns, especially under relatively wet conditions (Calder, 1998). Under drier conditions, aspects of water supply, dictated in part by root extent, dominate over atmospheric water demand and help determine water use patterns by vegetation. The combination of deep root systems (Canadell et al., 1996), high aerodynamic rough-

ness (Calder, 1998) and low albedo (Jackson et al., 2008) of forests usually allow them to maintain higher evapotranspiration rates and lower deep drainage fluxes in dry and wet conditions compared to herbaceous plants (Zhang et al., 2001).

The influence of vegetation on the partitioning of precipitation between wet (i.e., deep drainage and runoff) and dry (evapotranspiration) water fluxes controls water exchange with the atmosphere, streams, ground water, and the soil. Evapotranspiration, both as a component of the energy balance and a source of moisture to the atmosphere, may affect mesoscale circulation patterns and regional weather (Kelliher et al., 1993). Transpiration, the principal component of evapotranspiration over land, is tightly coupled with vegetation productivity in most ecosystems (Monteith, 1988). Deep drainage is the main water source that feeds groundwater bodies and, together with surface runoff, determines the water yields of watersheds. Changes in plant cover affecting the balance of liquid and vapor water can have a strong impact on ecosystem functioning, with important consequences on ecosystems services such as water, food, and hydroelectric power provision as well as hydrological and climatic regulation.

* Corresponding author at: Grupo de Estudios Ambientales, Instituto de Matemática Aplicada San Luis, Universidad Nacional de San Luis & CONICET, Av. Ejército de los Andes 950, 5700 San Luis, Argentina. Tel.: +54 2652 422803; fax: +54 2652 422803.

E-mail address: marcelo.nosetto@gmail.com (M.D. Nosetto).

The effects of changes in plant cover on hydrological processes have been studied globally using various approaches and different plant transitions. Transitions between tree- and herbaceous-dominated covers, which are taking place at increasing rates in South America (Paruelo et al., 2006), have shown the greatest impact on the water balance (Farley et al., 2005). For instance, native forest clearing for crop production in Australia and the Sahel has led to increased groundwater recharge and a raising of water-table levels because of the lower evapotranspiration rates of croplands (Schofield, 1992; Leblanc et al., 2008). In the opposite case, grassland afforestation usually increases evaporative water fluxes and reduces water yields (Farley et al., 2005; Noretto et al., 2005). Transitions between structurally similar vegetation types, such as tree plantations from native forests or from grasslands to crops, have received much less attention, although the hydrological impacts could be large.

Tree plantations and crops are expanding rapidly in temperate South America, including Argentina, Uruguay and Paraguay. In Argentina, the area covered by annual crops increased at a rate of 0.27% per year between 1988 and 2002 (Paruelo et al., 2006), with 21 million hectares devoted to the production of rain-fed soybeans, wheat, maize, and other grains nowadays (MAGP, <http://www.minagri.gob.ar/>). Similarly, rates of land conversion to tree plantations, particularly fast-growing species such as eucalypts and pines, jumped from 23,000 to 125,000 ha per year during the 1992–2001 period (SAGPyA, 2002). The native grasslands of the Pampas and the native dry forests of the Espinal and Chaco districts have been the primary source of these expansions (Paruelo et al., 2006). Facing a rising global demand for food and fiber, a further expansion of croplands and afforestations seems likely. In addition to the direct economic benefits, the hydrological consequences of such vegetation changes should be considered for land-use planning, particularly in the context of an increasing frequency and intensity of extreme climatic events (drought and flooding) that could magnify vegetation change impacts (Viglizzo and Frank, 2006).

In this paper, we explore the hydrological effects of replacing native grasslands and native dry forests with crops, such as soybean and wheat/soybean systems, and eucalyptus plantations. We focus on the transition zone between the Pampas and the Espinal districts in temperate Argentina (Cabrera, 1976), where remaining patches of native grasslands and forest coexist with growing areas of grain crops and eucalypt plantations. We evaluated evapotranspiration patterns first for the 2000–2001 growing season in 60 plots of native grasslands, native forests, eucalyptus plantations, and annual crops, including soybean and wheat/soybean rotations, based on the thermal information provided by 13 Landsat images. We complemented these data with long-term estimates (11 years, 1994–2004) of water fluxes, including transpiration, soil evaporation and deep drainage, based on a water balance model (HYDRUS 1D, Šimůnek et al., 2005). Additionally, we characterized soil moisture profiles in detail at one location that encompassed adjacent stands of native grassland, dry forest, eucalyptus plantation, soybean and wheat/soybean system.

2. Materials and methods

2.1. Study region

We performed our study in the transition area between the Pampas and the Espinal districts in the Entre Ríos province (Argentina, Fig. 1). The study region lies between latitudes -32.11° and -31.69° and longitudes -60.57° and -60.06° . The area has a rolling landscape, with elevation that varies between 30 and 110 m a.s.l. The climate is humid temperate and the mean annual temperature is $\sim 18.5^\circ\text{C}$. Mean temperatures for the coldest (July) and



Fig. 1. Location of the study region showing the original grassland distribution of the Pampas (light gray) and the original dry forests of the Espinal and Chaco districts (dark gray).

warmest (January) months are 12.4°C and 25°C , respectively. Mean annual rainfall is 1100 mm and it has a summer-dominant distribution, with 65% of which occurs during spring and summer (October–March). Mean annual potential evapotranspiration (Penman–Monteith) is 1150 mm and 71% of it occurs during spring and summer. The rolling landscape together with relatively high rainfall has led to a high density of rivers and streams in the area. Soils in the area developed from loessic materials and are dominated by Mollisols ($\sim 85\%$) and Vertisols (12%) in a lesser extent. Among Mollisols, *Acuic Argiudol* is the dominant soil subgroup, followed by *Vertic Argiudol* but in much less proportion. These soils are well drained and have a silt–loam or silty–clay–loam texture in the surface layers. Clay content in the surface layer is usually between 25% and 30%. Iron and manganese mottles and calcium carbonate concretions may be found in the soil profile. Organic matter content varies between 2% and 4% in the surface layer (INTA, 1998).

Since our study region is located in the transition zone between the grasslands of the Pampas and the dry forests of the Espinal district (Fig. 1), remaining patches of both covers could still be found in the area, but they are being converted to croplands at rapid rates (Paruelo et al., 2006). Although it is not very certain, the limit between both phytogeographical districts seems to be related with a climate switch towards a negative water balance during part of the year; conditions that favor the competitive ability of the grasses (Soriano et al., 1991). An alternative hypothesis suggests that a high fire frequency during the pre-Columbian time destroyed original scrubs and forests, promoting the prevalence of grasses in the Pampas (Soriano et al., 1991). *C3* and *C4* grasses of the genera *Paspalum*, *Axonopus*, *Stipa*, *Bromus*, and *Piptochaetium* dominate the grassland areas, while trees of the genera *Prosopis*, *Acacia*, *Jodina*, *Celtis*, *Schinus*, *Geoffroea* are the most common components of the dry forests. Currently, most of the study area is devoted to the rain-fed production of soybean (*Glycine max* L.), wheat (*Triticum aestivum* L.), maize (*Zea mays* L.) and sunflower (*Helianthus annuus* L.). Average yields of soybean and wheat, the two dominant crops, are 2.5 and 3 tonnes ha^{-1} (SAGPyA), respectively. Eucalyptus plantations are not a dominant vegetation cover, but the afforested area in the whole province of Entre Ríos now approaches 90,000 ha and

is growing rapidly (Braier, 2004). A prospective carbon sequestration market and an increasing demand for wood products is likely to continue the rapid expansion of this land-use option.

2.2. Satellite estimates of evapotranspiration

We evaluated the influence of vegetation cover on evapotranspiration (ET) based on Landsat data. We selected 60 plots, each >10 ha in size, occupied by native dry forests ($n=17$), native grasslands ($n=10$), eucalyptus plantations ($n=6$), repeated soybean cultivation (one crop per year, $n=11$) and wheat/soybean rotation (two crops per year, $n=16$). All tree plantations were >15 years of age. To avoid edge effects on the data from satellite images, we used core pixels at each plot excluding a ~60 m-wide edge zone.

We used 13 Landsat 7 ETM+ images (scenes 226/82 and 227/82) that cover our study region. Selected images encompassed the whole 2000/2001 growing season and were acquired at 10:30 h (local time) on June 25, July 27, September 6, November 16, and December 2 and 18 of year 2000 and January 12, February 4 and 20, March 8, April 2 and 26, and June 28 of year 2001. Landsat images were downloaded from the Earth Resources Observation and Science (EROS) Center using the USGS Global Visualization Viewer tool (<http://glovis.usgs.gov/>). To minimize atmospheric effects, non-thermal bands were corrected using a dark object subtraction (DOS) as described by Chavez (1989). The thermal band was corrected using the mono-window algorithm proposed by Qin et al. (2001).

We estimated actual daily ET using surface radiant temperature measurements based on the so-called “simplified method” (Carlson et al., 1995). This method has a strong physical basis and has been successfully applied for different vegetation types (crops, grasslands, and forests). In this approach, actual daily ET is calculated considering the net radiation received by the surface and its temperature difference with the surrounding air mass based on the following equation (Carlson et al., 1995):

$$ET_{24} = Rn_{24} - b(T_s - T_a)^n \quad (1)$$

where ET_{24} (mm day^{-1}) and Rn_{24} (mm day^{-1}) are the integrated actual ET and net radiation over a 24 h period, respectively, T_s (K) is the surface radiant temperature, T_a (K) is the air temperature, and b ($\text{mm day}^{-1} \text{K}^{-1}$) and n are parameters derived from NDVI that vary with vegetation type. Since stress factors like soil moisture deficit, soil salinity or plant diseases are implicitly captured by the surface temperature, albedo and NDVI, the evapotranspiration estimates derived with this approach correspond to actual values of evapotranspiration.

Net radiation (Rn), which arises from the sum of the net short-wave and net long-wave components, was computed from meteorological data registered in a station located at the geographic center of the study area. Albedo values were derived from Landsat imagery according to Liang (2000). The incoming short-wave radiation measured in the meteorological station and the albedo data were used to compute the net short-wave radiation. The net long-wave radiation was estimated from air temperature, humidity and solar radiation according to Allen et al. (1998). Temperature difference estimates ($T_s - T_a$) were based on the surface temperature (T_s), derived from band 6 of Landsat images according to the algorithm proposed by Qin et al. (2001), and the air temperature (T_a) measured at the meteorological station. The “ b ” coefficient represents an average bulk conductance for daily-integrated sensible heat flux and the “ n ” coefficient is a correction for non-neutral static stability. Both coefficients were obtained from a scaled vegetation index ($NDVI^*$) computed from bands 3 and 4 of Landsat images according to the procedure described by Carlson et al. (1995). The effects of vegetation cover on evapotranspiration rates were analyzed using one-way analysis of variance (ANOVA), followed by Duncan's test.

Table 1

Structural and functional characteristics of the different vegetation covers simulated in HYDRUS 1D.

	Maximum rooting depth (m)	Annual potential transpiration (mm y^{-1})	Annual potential evaporation (mm y^{-1})
Native forests	4	1040	162
Native grasslands	2	758	233
Tree plantations	4	1077	144
Soybean	1.8 (1.15)	654	280
Wheat/soybean	1.8 (0.63)	804	236

Maximum rooting depth was set constant throughout the simulation period in native forests, grasslands and tree plantations but varied for annual crops (see Section 2). The bracketed values showed the annual average maximum rooting depth.

2.3. Soil water modeling

To complement the satellite estimates of ET, we used the HYDRUS 1D software (Šimůnek et al., 2005) to simulate the effect of vegetation cover on soil water dynamics. HYDRUS 1D simulates water, heat, and solute transport in one-dimensional, variably-saturated media. Water flow modeling is based on the Richard's equation and incorporates a sink term to account for water uptake by plant roots (Feddes et al., 1978). This model has been successfully used in numerous hydrological studies and under different climatic and agricultural conditions.

In this study, we defined a flow domain of 4 m of depth encompassing six soil layers, corresponding to a typical Mollisol profile of the study region (INTA, 1998). We chose a typical Mollisol profile for the modeling experiments since this is the dominant soil type of the study area (~85% of areal coverage in the region) and the target of most of the agricultural expansion (INTA, 1998). This soil developed on loessic sediments and has a silty-loam texture. In the surface layers, organic matter approaches 2.5% and the texture is silty-clay-loam. Ground water is usually deeper than 20 m (INTA, 1998). Hydraulic properties of van Genuchten's function (1980) were determined with the pedo-transfer functions of Rosetta software (Schaap et al., 2001) based on sand-silt-clay contents. Pedotransfer functions in Rosetta were developed from more than 2000 soil samples, with a large proportion of them corresponding to the same soil textural class of the soil profile we modeled. Because of the lack of cracks and fractures in these soils, we used the van Genuchten's model (van Genuchten, 1980) of hydraulic properties instead of a dual-permeability model. Daily values of precipitation, potential transpiration and potential evaporation were defined as upper boundary conditions, and free drainage was allowed at the lower boundary. A simple rainfall interception model, relating interception loss to the surface leaf area index, is applied in HYDRUS (Šimůnek et al., 2005). Surface runoff fluxes were estimated with the curve-number method (USDA, 1986) and were subtracted from rainfall inputs. The hydrological soil group D (silty-clay-loam texture) was used for the calculation, while the runoff curve numbers for each vegetation cover were obtained from USDA (1986). Simulations involved the repetition of an 11-year period (1994–2004). The first run was initiated with intermediate soil moisture levels (intermediate between field capacity and wilting point) and its final moisture levels were used as the initial conditions for the second run, which was the only one considered in our analysis of the results.

The effects of vegetation cover on water dynamics were considered in HYDRUS by changing the maximum rooting depth, potential transpiration, and potential evaporation on modeling exercises (Table 1). We defined the maximum rooting depth of native forests, grasslands and tree plantations according to previous research (Noretto, 2007) and direct observations of soil profiles in the field. For native forests, grasslands, and tree plantations, we used a

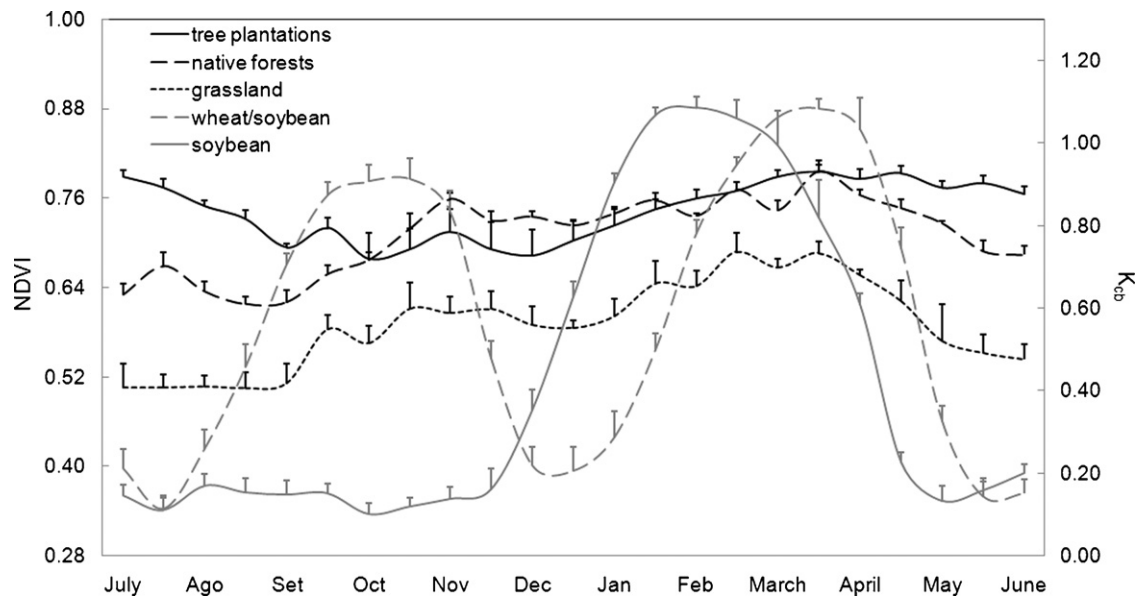


Fig. 2. Seasonal dynamics of NDVI and Kcb (basal crop coefficients used for transpiration scaling) for different vegetation covers. Kcb values were obtained by scaling NDVI values from MODIS imagery between minimum and maximum Kcb values of 0.1 and 1.15, respectively, and then corrected for vegetation height, air humidity and wind speed. NDVI was characterized from MODIS images for the period 2001–2003 in plots occupied by native dry forests ($n=7$), native grasslands ($n=5$), eucalyptus plantations ($n=6$), soybean ($n=14$) and double wheat/soybean system ($n=13$). See Section 2 for additional details.

constant maximum rooting depth throughout the whole simulation period. We considered variable rooting depths for annual crops, with maximum rooting depth increasing at a rate of 0.18 cm per degree-day from 0.1 m at sowing to a maximum value of 1.8 m (Dardanelli et al., 2008). In this calculation, we used a base temperature (above which degree-days are counted) of 7.8 °C and 0 °C for soybean and wheat, respectively (Dardanelli et al., 2008). Root distributions were assumed to decline linearly from the surface to the maximum rooting depth in all vegetation covers. The van Genuchten's (1987) function was used as root water uptake model.

Potential transpiration and potential evaporation were determined as the product between the reference potential evapotranspiration (E_{To}) and the basal crop coefficient (K_{cb}) and evaporation coefficient (K_e), respectively (Allen et al., 1998). Penman–Monteith potential evapotranspiration was determined from temperature, humidity, wind speed and solar radiation data (Allen et al., 1998). K_e values were computed according to Allen et al. (1998) using precipitation data as the main input. K_{cb} values were obtained scaling NDVI values from MODIS imagery between minimum and maximum K_{cb} values of 0.1 and 1.15, respectively, and then corrected for vegetation height, air humidity and wind speed (Allen et al., 1998) (Fig. 2). Potential transpiration, as well as potential evaporation, is transformed into actual values in HYDRUS by affecting it by a stress factor determined by soil moisture. No osmotic stress was considered in the modeling.

The NDVI index has proved to be highly correlated with net primary productivity and leaf area index. We characterized the seasonal pattern of NDVI in 45 plots occupied by native dry forests ($n=7$), native grasslands ($n=5$), eucalyptus plantations ($n=6$), soybean ($n=14$) and double wheat/soybean system ($n=13$). For the period 2001–2003, we used the MOD13Q1 product (Collection 5), which derives from the daily surface reflectance product (MOD09 series), corrected for molecular scattering, ozone absorption, and aerosols. It represents a 16-day composite with a pixel size of 250 m. Subsets of the images of the study region were downloaded from Oak Ridge National Laboratory (<http://daac.ornl.gov/>). Tree plantations showed the highest mean annual K_{cb} value (0.88) followed by native forests (0.82), grasslands (0.59), double wheat/soybean

system (0.61), and soybean (0.44). Crop systems showed a typical seasonal pattern of highest K_{cb} values (~ 1) during the peak of the growing season and minimum values (~ 0.15) during the fallow period (Fig. 2).

2.4. Soil sampling for moisture assessment

To provide an independent characterization of land cover effects on hydrological properties, we selected nearby five stands occupied by native forests, grasslands, eucalyptus plantation, soybean and double-cropped wheat/soybean system where mineral soils were sampled for moisture analysis. All stands were located on the same topographic position and shared the same soil type, as confirmed by direct observation in the field. Soils, developed from calcareous loess, are Acuic Argiudols, moderately drained and with a silty-clay-loam texture in the top horizon. Clay content in the top layer ranges from 28% to 32%. No shrinking–swelling signs were observed at this site. As evidenced from soil chemical analysis (data not shown), there were no salinity/sodicity problems and topographic slopes were <0.5%.

The native forest stand was 3 ha in size and was dominated by species of the genera *Prosopis*, *Geoffroea*, *Celtis* and *Acacia*. Current tree density approached ~ 3800 trees ha^{-1} and basal area was $35 m^2 ha^{-1}$. Tree height approached ~ 4 m and the understory was sparse. The 3-ha grassland stand was typically grazed and was dominated by species of *Stipa*, *Bromus*, *Piptochaetium* and *Paspalum*. It was neither fertilized nor irrigated. The eucalypt plantation, which was established in 1976 and was 33 years of age at the time of our measurements, was originally a native dry forest. The plantation was 2 ha in size and was never harvested, fertilized, or irrigated. Current tree density approached ~ 760 trees ha^{-1} , tree height ~ 28 m, and basal area $65 m^2 ha^{-1}$. An understory was absent. Wheat/soybean (13 ha in size) and soybean (7 ha) stands were also originally dry forests but have been planted as crops for at least 50 years. No-tillage management is widespread in the region and was used in both stands. Weeds were controlled with herbicides, particularly glyphosate. Stands are usually weed-free managed throughout the whole seasons.

Table 2

Thermal, radiometric, and evapotranspirative characteristics obtained from Landsat images for different vegetation covers.

	n	Ts–Ta (°C)		Albedo		ET (mm d ⁻¹)	
		Mean	SD	Mean	SD	Mean	SD
Tree plantations	6	1.66 c	0.54	0.17 a	0.025	3.12 a	0.25
Native forests	17	1.59 c	0.46	0.17 a	0.008	3.17 a	0.20
Grasslands	10	3.73 b	0.53	0.22 b	0.014	2.13 b	0.16
Wheat/soybean	16	4.28 b	0.49	0.22 b	0.013	2.21 b	0.12
Soybean	11	5.44 a	0.79	0.24 c	0.013	1.85 c	0.16

Mean and standard deviation (SD) of temperature differences between the surface and the air (Ts–Ta), albedo and actual evapotranspiration rates (ET) computed from 13 Landsat images. The mean values were obtained by averaging the thirteen dates analyzed. Letters show significant differences ($p < 0.05$) among vegetation covers (Duncan's test). The number of plots is indicated (n).

Soil samples, taken in December 2009, were collected to a depth of 3 m (0–25, 25–50, 50–100, 100–150, 150–200, 200–250, and 250–300 cm). At each stand we randomly located three soil pits. Soil sampling points were spaced ~10–15 m apart and ~40 m from fences to avoid edge effects. In forest plots, soil sampling points were >1 m from tree stems. Soil samples were taken with a hand-auger (10-cm outside diameter). Full samples from each depth interval were immediately mixed in the field, sub-sampled and stored in double plastic bags for moisture analysis. Moisture content was determined gravimetrically one to three days after sampling (oven drying method, Gardner, 1986) and then converted to volumetric moisture by multiplying by the bulk density. Particle size distribution, determined by the hydrometer method (Bouyoucos, 1962), and gravimetric moisture were used to provide estimates of bulk density (Vervoort et al., 2006). Moisture contents were analyzed with one-way ANOVA and multiple comparisons were performed with Duncan's test.

3. Results

3.1. Evaporative water fluxes

Vegetation cover exerted a strong influence on evapotranspiration, as demonstrated by the analysis of 13 Landsat images (Table 2). Despite strong structural differences between eucalyptus plantations and native dry forests, these two vegetation types displayed remarkably similar ET values that were significantly higher than those of herbaceous plots in our study. On average at the annual scale, tree-dominated land covers used ~50% more water than the grassland or cropland plots (3.1 mm d⁻¹ compared with 2.1 mm d⁻¹, respectively). Across all plant types, the maximum dif-

ference in evapotranspiration was for the native forests compared to soybeans (1.7 times greater in the forest), the dominant land-use transformation in the region currently. Within herbaceous covers, grasslands and the wheat/soybean double-crop system showed similar ET values ($p > 0.10$) but were 17% higher than for the single-soybean crop system.

Tree plantations and native forests had the highest ET values computed from Landsat imagery at all analyzed dates (Fig. 3). However, ET rates of tree-dominated covers were not significantly different from the wheat/soybean system at the end of winter nor were they different from the single soybean system in the middle of summer, denoting the high evapotranspiration capacity of grain crops at the peak of their growing seasons. Small differences were observed between tree plantations and native forests across the growing season. While in the spring the native forests evapotranspired ~10% more water than tree plantations ($p < 0.05$), in winter the pattern reversed and tree plantations used ~5% more water ($p < 0.10$).

Herbaceous vegetation types displayed a 35% higher albedo than tree-dominated covers (Table 2). This result implies an extra radiant energy input of ~1 MJ m⁻² for the latter, on average annually. Despite this additional energy input, tree-dominated covers had canopies that were ~3 °C cooler than for the herbaceous vegetation (1.6 compared with 4.5 °C, respectively), evidence of a higher capacity of heat transfer from canopies to the atmosphere in tree-dominated covers.

The HYDRUS modeling provided insight into the partitioning of ET between transpiration and evaporation. Seasonal transpiration patterns derived from HYDRUS followed the seasonality of vegetation cover (Figs. 2 and 4), with maximum rates at the leaf area peaks during the growing seasons. Maximum transpira-

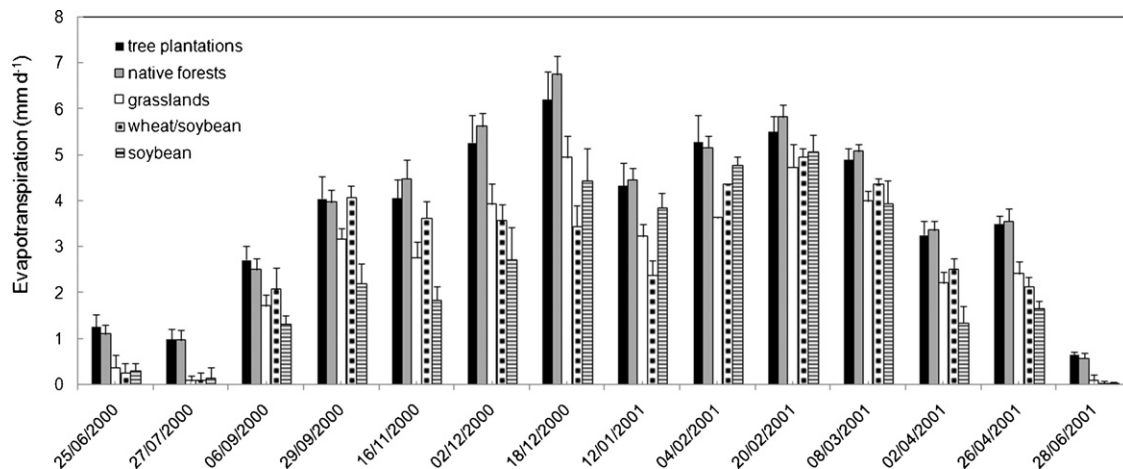


Fig. 3. Actual evapotranspiration estimated from Landsat images for different vegetation covers on thirteen dates. The selected plots were each >10 ha in size and represented native dry forests (n = 17), native grasslands (n = 10), eucalyptus plantations (n = 6), continuous soybean cultivation (n = 11) and wheat/soybean rotation (n = 16). Daily evapotranspiration was estimated from Landsat 7 ETM+ images (scenes 226/82 and 227/82). Lines above bars indicated the standard deviation.

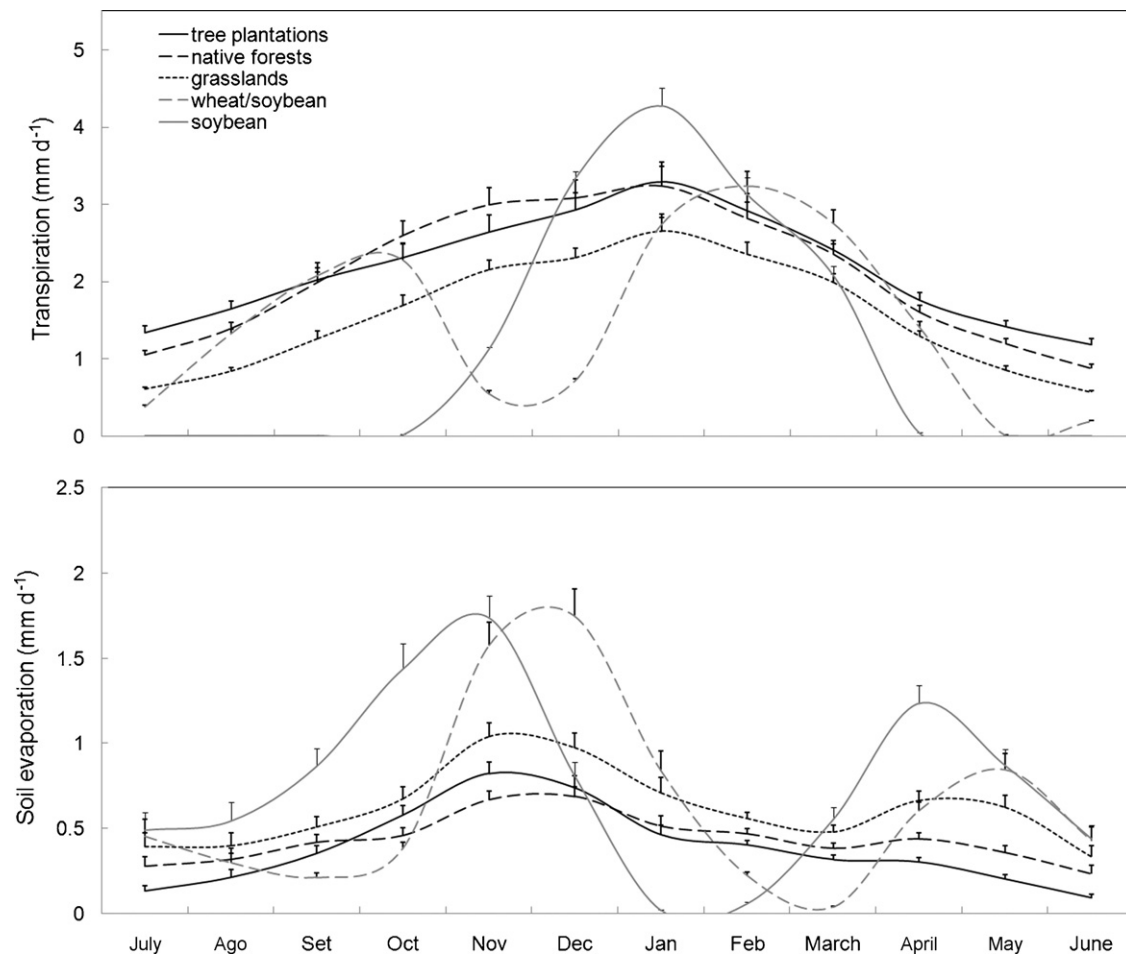


Fig. 4. Modeled seasonal pattern of daily transpiration and soil evaporation for different vegetation covers. Monthly averages and standard deviations for eleven years of simulation (1994–2004) with HYDRUS 1D are also shown.

tion rates were predicted in spring for native forests (2.9 mm d^{-1}) and in summer for tree plantations (2.9 mm d^{-1}), in agreement with Landsat-based ET patterns. For all herbaceous covers, maximum transpiration rates were also observed in summer (2.3 , 2.9 and 3.1 mm d^{-1} for grasslands, wheat/soybean and soybean). Two sharp transpiration peaks (2.3 mm d^{-1} in October and 3.2 mm d^{-1} in February) were evident in the wheat/soybean system, which corresponded to the peaks of leaf area for wheat and soybean growing seasons, respectively, as suggested by NDVI patterns (Fig. 2). At the annual scale, maximum transpiration amounts were predicted for tree-dominated covers (785 and 764 mm y^{-1} for tree plantations and dry forests, respectively), followed by grasslands (562 mm y^{-1}), wheat/soybean double crop system (533 mm y^{-1}) and soybean single crop (423 mm y^{-1}). These amounts accounted for 37% (soybean) to 69% (tree plantations) of total ecosystem water fluxes (Fig. 5).

Annual soil evaporation amounts derived from HYDRUS were the greatest for soybean (275 mm y^{-1}), followed by wheat/soybean and grasslands ($\sim 230 \text{ mm y}^{-1}$) and tree-dominated covers ($\sim 150 \text{ mm y}^{-1}$). The highest soil evaporation rates were observed at the end of spring (November and December) for all vegetation covers ($\sim 1 \text{ mm d}^{-1}$ on average), mainly responding to high rainfall inputs (290 mm) and atmospheric water demands ($\sim 5 \text{ mm d}^{-1}$). A second soil evaporation peak was observed in autumn only in herbaceous covers ($\sim 0.8 \text{ mm d}^{-1}$ on average), driven by high rainfall amounts (250 mm) and low plant cover. Interception losses accounted for a small fraction of total fluxes, approaching $\sim 4.5\%$ in tree-dominated covers and 2.5% in herbaceous ones (Fig. 5).

3.2. Liquid water fluxes

Despite lower rainfall inputs, the highest simulated drainage fluxes took place in winter for all vegetation covers, except in the soybean-only system ($\sim 0.3 \text{ mm d}^{-1}$, on average, Fig. 6). The

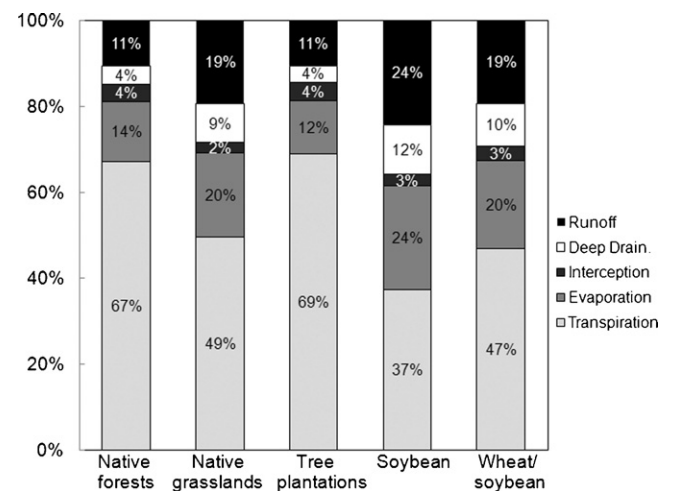


Fig. 5. The partition of ecosystem water fluxes for different vegetation covers. Values were obtained by averaging eleven years of simulations. Water fluxes were modeled with HYDRUS 1D, with the exception of runoff, which was obtained with the Curve Number method (see Section 2).

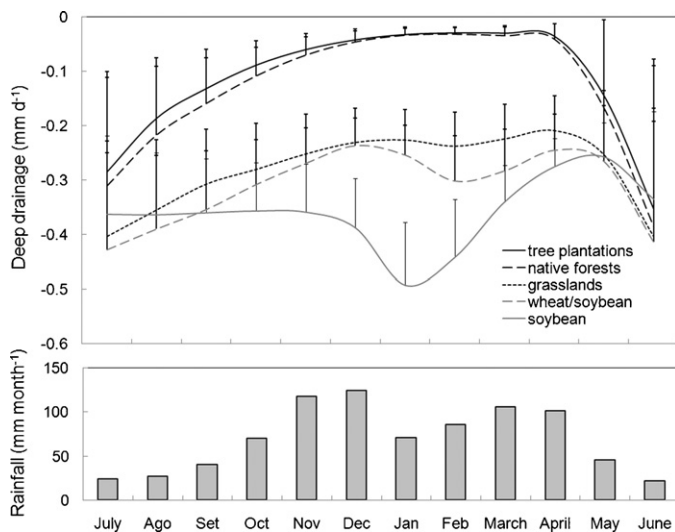


Fig. 6. Seasonal patterns of rainfall and deep drainage flux for different vegetation covers. Monthly rainfall was obtained from a meteorological station located in the study region (period 1994–2004). The average and standard deviation of deep drainage were modeled with HYDRUS 1D.

low atmospheric water demand of this season has likely favored water replenishment of soil profiles and deep drainage fluxes. Under soybean, a deep drainage peak was observed in summer ($\sim 0.5 \text{ mm d}^{-1}$), likely driven by the high rainfall inputs and low transpiration rates of the previous months (Fig. 6). Excluding two years with extreme rainfall events ($>200 \text{ mm}$ in a week), deep drainage represented less than 1% of total ecosystem fluxes in tree-dominated covers, $\sim 6\%$ in grasslands and wheat/soybean and $\sim 9\%$ in soybean. Simulated deep-drainage fluxes increased to 18% of total water fluxes in woody covers and 25% in herbaceous ones during the wet 2003 year (Fig. 5). On average, annual deep drainage fluxes approached $\sim 45 \text{ mm y}^{-1}$ in woody covers, $\sim 105 \text{ mm y}^{-1}$ in grasslands and wheat/soybean and 135 mm y^{-1} in soybean.

Surface runoff was an important component of the water balance, likely because of the fine texture of surface soil layers and a rainfall pattern with intense rainfall events. Maximum simulated runoff amounts were estimated for soybean, where it approached 270 mm y^{-1} (24% of total water fluxes), followed by grassland and wheat/soybean, with $\sim 220 \text{ mm y}^{-1}$, and woody covers, with 120 mm y^{-1} (Fig. 5).

Deep soil profiles for all vegetation types at one location provided support for the satellite-derived evapotranspiration estimates and modeling outputs. Moisture profiles showed significantly drier soils in tree-dominated covers compared to herbaceous ones (Fig. 7, $p < 0.05$), suggesting higher water use in the former. The average moisture content, weighted by the thickness of each soil layer, showed that soil profiles under tree-dominated covers had one-eighth less volumetric water content ($0.31 \text{ m}^3 \text{ m}^{-3}$) than wheat/soybean profiles ($0.35 \text{ m}^3 \text{ m}^{-3}$) and one-fifth less than grassland and soybean profiles (0.39 and $0.38 \text{ m}^3 \text{ m}^{-3}$, respectively). Differences between woody and herbaceous covers in the total amount of water stored to 3 m depth approached $\sim 190 \text{ mm}$. Water stored at deep soil layers (2–3 m of depth) showed close agreement with modeling estimates, with a mean root square error of $<30 \text{ mm}$.

4. Discussion

Transitions in vegetation cover led to profound hydrological changes, particularly for shifts between herbaceous and tree-dominated vegetation. The combination of satellite analysis, soil water modeling, and moisture profiles confirmed the greater evap-

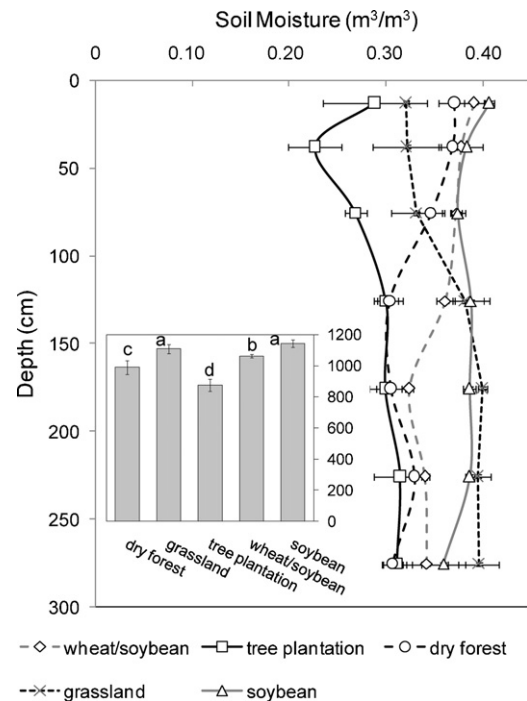


Fig. 7. Water content profiles in the soil under different vegetation covers. The average and standard deviation of volumetric water content at one location is shown ($n = 3$ per stand). The inset graphic shows total accumulated soil water down to the maximum sampled depth of 3 m. Letters show significant differences ($p < 0.05$) among vegetation covers (Duncan's test).

otranspirative capacity of woody covers. This result may arise from a suite of features for trees that includes deeper root systems (Canadell et al., 1996), extended growing seasons (Fig. 2), higher gaseous exchange capacity because of higher aerodynamic conductances (Kelliher et al., 1993), greater direct interception of precipitation, and higher inputs of radiant energy because of lower albedos (Table 2). The similarity of seasonal maximum evapotranspiration rates between tree-dominated covers and grain crops (Figs. 3 and 4) highlighted the importance of the gaseous exchange capacity and points to other evapotranspirative constraints in herbaceous vegetation. Since albedo change only explains $\sim 18\%$ of the difference in evapotranspiration (Table 2), roots pattern and leaf area seasonality are likely playing a major role, as suggested by soil moisture values at deep soil layers (Fig. 7) and by the seasonal variation of NDVI and transpiration rates (Figs. 2 and 4). These results suggest a combined control of both water demand and supply on evapotranspiration of herbaceous vegetation (Calder, 1998).

The different approaches we used to estimate the hydrological parameters yielded convergent results, providing greater confidence in our conclusions. Annual evapotranspiration estimates showed good agreement between the satellite analysis and HYDRUS modeling (root mean square error = 32 mm y^{-1}). Water use estimates for the single soybean crop and double wheat/soybean crop in the region approach 500–600 mm and 750–900 mm during their growing season, respectively (Totis de Zelijkovich et al., 1991; Andriani, 2000). These figures compare well with our satellite (570 mm for soybean and 737 mm for wheat/soybean) and modeling estimates (510 mm for soybean and 740 mm for wheat/soybean).

Modeling estimates of water yield (runoff + deep drainage) also showed good agreement with hydrometric measurements performed in a watershed close to our study region. The average water flow of Nogoyá river for the 1990–2003 period averaged $29 \text{ m}^3 \text{ seg}^{-1}$ (Subsecretaría de Recursos Hídri-

cos, <http://www.hidricosargentina.gov.ar>), which corresponds to a water yield of 220 mm y^{-1} (watershed area = 4200 km^2). A rough land-cover assessment of the watershed, based on Landsat images, suggests that for the year 2000 the proportion of grasslands, woody covers, wheat/soybean and soybean approached 0.22, 0.40, 0.26 and 0.12, respectively. Using these proportions and modeling outputs we estimated an average water yield of 255 mm y^{-1} . The seasonal pattern of both approaches also showed a good agreement when modeling estimates were delayed by one month to account for the time of concentration of the watershed ($r^2 = 0.45$, $p < 0.05$, $n = 12$ months). A rough lineal extrapolation suggests that if half of the remaining grasslands and woody covers (1300 km^2) of this watershed are converted to soybean the annual water yield will only be increased by 20% (from 255 to 307 mm y^{-1}).

The strongest hydrological contrasts were manifested between dry forests and the single crop of soybean, which is the dominant land-use transformation occurring in the study region and in other dry forests of Argentina today (Gasparri and Grau, 2009). Tropical and temperate dry forests are one of the most endangered ecosystems worldwide, and the Espinal and Chaco districts of Argentina are no exception. In recent decades, dry forest deforestation rate in the region approached $200,000 \text{ ha y}^{-1}$ (UMSEF, 2008), motivated in part by the global soybean market, technological improvements, and a trend in increasing rainfall. According to our analysis, the replacement of dry forests by soybean would cut evapotranspirative water fluxes by one third and would almost triple deep drainage fluxes (Table 2). In this context, it is worth comparing the Australian situation where the replacement of native dry forest by rainfed annual crops and pastures in both winter- and summer-dominant rainfall areas more than a century ago increased groundwater recharge, raising water-tables and moving deeply stored salts to the surface (Schofield, 1992). Because of this hydrologic change, Australia has lost thousands of hectares of productive agricultural lands (George et al., 1999). A similar process is also taking place in the Sahel plains, although without salinization (Leblanc et al., 2008), and initial stage of this process could be also taking place in the Great Plains of North America (Scanlon et al., 2005). Whether this process is already beginning in South American countries such as Argentina and Paraguay, where agricultural expansion is recent, is still uncertain; however such an occurrence is likely in the future based on our results and some sparse hydrological measurements that suggest rising groundwater levels (Jobbágy et al., 2008) and leaching of a large stock of salts in dry forest converted to agriculture (Santoni et al., 2010).

Preferential water flow through soil macropores, such as root channels, was not considered in our modeling exercises, although it may be influenced by vegetation cover. Because of higher root density, microfaunal activity and/or content of soil organic matter and litter, afforestation may improve the porosity and capacity of water transport of soils, particularly in fine-textured ones (Noretto et al., 2007). These changes would likely lead to improved infiltration and deep drainage, reduced runoff and soil erosion and eventually the leaching of soluble vadose salts, as it has been observed after afforestation of fine-textured sodic soils in the Hungarian plains, Caspian region and India (Sizemskaya and Romanenkov, 1992; Mishra and Sharma, 2003; Noretto et al., 2007).

Besides the strong hydrological changes generated by woody–herbaceous transitions, less obvious vegetation changes, such as the replacement of grasslands by crops or cultivating two crops in a year (double wheat/soybean) instead of one crop (soybean alone), could also lead to noticeable hydrological alterations. While the replacement of grasslands by the double wheat/soybean crop would lead to minor hydrological changes, the use of the single soybean crop would significantly reduce evapotranspiration and increase liquid water flow (Table 2, Figs. 5 and 6). In the Inland Pampas of Argentina, the widespread replacement of pastures

and grasslands by annual crops, which took place primarily in recent decades, has been linked to an increase of flooding events, as suggested by historical water-table levels and land-use patterns (Viglizzo et al., 2009). At the regional scale, the liquid water excesses generated by the new land-use would be hard to evacuate from the region because of the flat topography of the landscape (regional slopes $< 0.1\%$) and the lack of rivers and streams (Noretto et al., 2009; Aragón et al., 2010). Instead this liquid water would enhance recharge and raise groundwater levels, potentially triggering flooding (Aragón et al., 2010). Although this hypothesis is still preliminary, the results of our study are consistent with this possibility.

The hydrological changes triggered by land-use shifts could entail positive or negative impacts on water services depending on where the changes take place. For instance, afforestation in flooding-prone landscapes like the flat Inland Pampas could be beneficial, decreasing the risk of flooding and helping to deepen groundwater levels because of the higher evapotranspirative capacity of trees (Table 2; Noretto et al., 2008). For the same reason, however, afforestation in subhumid and semiarid regions, such as the Sierras Pampeanas rolling hills or NW Patagonia, could be detrimental if it decreases water yield (Farley et al., 2005) and jeopardizes other water uses. In the opposite case, the replacement of dry forests by agriculture could improve water yields, but at the same time, could promote the rise of water table levels and put agricultural lands at greater risk of flooding and salinization (Jobbágy et al., 2008). According to our modeling estimates, for instance, the replacement of dry forest by double cropping would double the annual water yield (from 154 to 312 mm y^{-1}) and decrease the seasonal variability (from 68% to 54% coefficient of variation of monthly water yield).

The contrasting evapotranspiration patterns among land uses offer land managers different options for regulating the water balance biologically. Since the rate of replacement of pastures and grasslands of the Inland Pampas with annual crops is unlikely to slow down, the potentially negative hydrological impacts of this land use transformation could be reduced if double cropping was implemented instead of the single crop system that prevails today or if tree plantations are incorporated in the landscape. According to our estimates, grasslands would be hydrologically similar to wheat/soybean double cropping or to mixed landscapes with three quarters of their area covered by single soybean crops and the rest by eucalyptus plantations. In the case of dry forest deforestation of the Chaco and Espinal districts of Argentina and Paraguay, the most likely biological avenue to restore the original hydrological conditions would be the reforestation of degraded lands, which become abandoned after few years of agriculture (Boletta et al., 2006). This strategy has been successfully applied in deforested areas of Australia, although estimates suggest that a large proportion of the landscape, perhaps as much as 70–80%, must be reforested to have a noticeable effect on regional groundwater levels (George et al., 1999).

An increasing global demand for food and biofuels requiring additional lands for agriculture and a prospective market for biologically sequestered carbon, suggest that land-use changes in Argentina are unlikely to cease in the near future. In this context, anticipating the likely outcomes of land-use change on water resources and proposing feasible ways to improve water yield and quality are desirable (Jackson et al., 2009). A climatic change scenario and the stochasticity of the processes that link climate, vegetation and hydrology add complexity to that task. In the Río de la Plata basin, the increased frequency of extreme climatic events or a likely reversal of current increasing rainfall trends may strongly impact water resources and ecosystem functioning, with negative consequences for food security. While assessing these impacts is one of the challenges to be faced in the region, an ecohydrological

perspective that explicitly considers the connections between climate, vegetation, and hydrology would be helpful for sustainable land use management in the region.

5. Conclusions

This research highlighted the strong effects of vegetation cover on hydrology and suggests likely avenues for hydrological regulation through land-use planning. Native grassland and dry forest areas of southern South America that are being intensively transformed into cropland could experience profound hydrological changes according to our results. Because of the lower evapotranspiration of single soybean cropping schemes, their massive expansion into the more evapotranspirative rangelands of the Pampas will impact surface and groundwater hydrology, likely increasing flooding risks; though these impacts could be lessened if the double wheat–soybean cropping scheme is implemented. However, the deepest impacts are expected to happen with tree–herbaceous transitions, such as the incipient spread of soybean into the dry forests of Chaco and Espinal districts of Argentina and Paraguay. In this case, decreased evapotranspiration, increased recharge, shallower groundwater levels and eventually salt mobilization are expected outcomes that may endanger agricultural lands, as it has been documented in Australia. These costs could be lessened, or at least delayed, if a thorough landscape planning, that must certainly include tree plantations, is implemented. However, solid policies that explicitly consider these hydrological contrasts will be required, together with a long-term monitoring scheme of key hydrological variables.

Acknowledgements

We wish to thank to Silvina Ballesteros and Ricardo Paez for their help during field and lab activities. We also acknowledge the comments and suggestions of two anonymous reviewers. This work was funded by grants from the Inter-American Institute for Global Change Research (IAI, CRN II 2031, supported by the US National Science Foundation, Grant GEO-0452325), the U.S. National Science Foundation (BIO-0717191), the International Development Research Center (IDRC - Canada) and the Agencia Nacional de Promoción Científica y Tecnológica (PRH 27).

References

- Allen, R.G., Pereira, L.S., Raes, D., Smith, M.D., 1998. Crop evapotranspiration. In: Guidelines for Computing Crop Water Requirements. FAO, Rome, p. 328.
- Andriani, J.M., 2000. El agua en los sistemas productivos. SAGPyA & INTA-EEA Oliveros. Para mejorar la producción, No. 13, Santa Fe, p. 72.
- Aragón, R.M., Jobbágy, E.G., Viglizzo, E.F., 2010. Surface and groundwater dynamics in the sedimentary plains of the Western Pampas (Argentina). *Ecohydrology*, doi:10.1002/eco.149.
- Boletta, P.E., Ravelo, A.C., Planchuelo, A.M., Grilli, M., 2006. Assessing deforestation in the Argentine Chaco. *For. Ecol. Manage.* 228, 108–114.
- Bouyoucos, G.J., 1962. Hydrometer method improved for making particle size analysis of soils. *Agron. J.* 54, 464–465.
- Braier, G.D., 2004. Tendencias y perspectivas del sector forestal al año 2020 Argentina. FAO/SAGPyA/SADS, Rome, p. 220.
- Cabrera, A.L., 1976. Regiones fitogeográficas argentinas. ACME, Buenos Aires, p. 85.
- Calder, I.R., 1998. Water use by forests, limits and controls. *Tree Physiol.* 18, 625–631.
- Canadell, J., Jackson, R.B., Ehleringer, J.R., Mooney, H.A., Sala, O.E., Schulze, E.D., 1996. Maximum rooting depth of vegetation types at the global scale. *Oecologia* 108, 583–595.
- Carlson, T., Capehart, W., Gillies, R., 1995. A new look at the simplified method for remote sensing of daily evapotranspiration. *Remote Sens. Environ.* 54, 161–167.
- Chavez Jr., P.S., 1989. Radiometric calibration of Landsat Thematic Mapper multispectral images. *Photogramm. Eng. Remote Sens.* 55, 1285–1294.
- Dardanelli, J., Collino, D., Otegui, M.E., Sadras, V.O., 2008. Bases funcionales para el manejo del agua en los sistemas de producción de los cultivos de grano. Producción de Granos – Bases funcionales para su manejo. Orientación Gráfica Editora, Buenos Aires, pp. 377–440.
- Farley, K.A., Jobbágy, E.G., Jackson, R.B., 2005. Effects of afforestation on water yield: a global synthesis with implications for policy. *Glob. Change Biol.* 11, 1565–1576.
- Feddes, R.A., Kowalik, P.J., Zaradny, H., 1978. Simulation of Field Water Use and Crop Yield. John Wiley & Sons Inc., New York, NY, p. 188.
- Gardner, W.H., 1986. Water content. In: Klute, A. (Ed.), Methods of Soil Analysis Part 1. American Society of Agronomy, Madison, pp. 493–544.
- Gasparri, N.I., Grau, H.R., 2009. Deforestation and fragmentation of Chaco dry forest in NW Argentina (1972–2007). *For. Ecol. Manage.* 258, 913–921.
- George, R.J., Nulsen, R.A., Ferdowsian, R., Raper, G.P., 1999. Interactions between trees and groundwaters in recharge and discharge areas—a survey of Western Australian sites. *Agric. Water Manage.* 39, 91–113.
- INTA, 1998. Carta de Suelos de la República Argentina. Departamento Paraná, Provincia de Entre Ríos. Relevamiento de Recursos Naturales. INTA, Paraná, p. 114.
- Jackson, R.B., Jobbágy, E.G., Nasetto, M.D., 2009. Ecohydrology in a human-dominated landscape. *Ecohydrology* 2, 383–389.
- Jackson, R.B., Randerson, J.T., Canadell, J., Anderson, R.G., Avissar, R., Baldocchi, D.D., Bonan, G.B., Caldeira, K., Diffenbaugh, N.S., Field, C.B., Hungate, B.A., Jobbágy, E.G., Kueppers, L.M., Nasetto, M.D., Pataki, D.E., 2008. Protecting climate with forests. *Environ. Res. Lett.* 3, doi:10.1088/1748-9326/1083/1084/044006.
- Jobbágy, E.G., Nasetto, M.D., Santoni, C., Baldi, G., 2008. El desafío ecohidrológico de las transiciones entre sistemas leñosos y herbáceos en la llanura Chaco-Pampeana. *Ecol. Aust.* 18, 305–322.
- Kelliher, F.M., Leuning, R., Schulze, E.D., 1993. Evaporation and canopy characteristics of coniferous forests and grasslands. *Oecologia* 95, 153–163.
- Leblanc, M.J., Favreau, G., Massuel, S., Tweed, S.O., Loireau, M., Cappelaere, B., 2008. Land clearance and hydrological change in the Sahel: SW Niger. *Glob. Planet. Change* 61, 135–150.
- Liang, S., 2000. Narrowband to broadband conversions of land surface albedo. I. Algorithms. *Remote Sens. Environ.* 76, 213–238.
- Mishra, A., Sharma, S.D., 2003. Leguminous trees for the restoration of degraded sodic wasteland in eastern Uttar Pradesh, India. *Land Degrad. Dev.* 14, 245–261.
- Monteith, J.L., 1988. Does transpiration limit the growth of vegetation or vice versa? *J. Hydrol.* 100, 57–68.
- Nasetto, M.D., 2007. Conversión de pastizales en forestaciones: Impacto sobre la dinámica del agua y las sales. Escuela para Graduados “Alberto Soriano”. Facultad de Agronomía, Universidad de Buenos Aires, Buenos Aires, p. 170.
- Nasetto, M.D., Jobbágy, E.G., Jackson, R.B., Szneider, G., 2009. Reciprocal influence between crops and shallow ground water in sandy landscapes of the Inland Pampas. *Field Crop Res.* 113, 138–148.
- Nasetto, M.D., Jobbágy, E.G., Paruelo, J.M., 2005. Land use change and water losses: the case of grassland afforestation across a soil textural gradient in Central Argentina. *Glob. Change Biol.* 11, 1101–1117.
- Nasetto, M.D., Jobbágy, E.G., Toth, T., Di Bella, C.M., 2007. The effects of tree establishment on water and salts dynamics in naturally salt-affected grasslands. *Oecologia* 152, 695–705.
- Nasetto, M.D., Jobbágy, E.G., Toth, T., Jackson, R.B., 2008. Regional patterns and controls of ecosystem salinization with grassland afforestation along a rainfall gradient. *Glob. Biogeochem. Cycles* 22, GB2015, doi:10.1029/2007GB003000.
- Paruelo, J.M., Guerschman, J.P., Piñeiro, G., Jobbágy, E.G., Verón, S.R., Baldi, G., Baeza, S., 2006. Cambios en el uso de la tierra en la Argentina y Uruguay: Marcos conceptuales para su análisis. *Agrociencia* 10, 47–61.
- Qin, Z., Karnieli, A., Berliner, P., 2001. A mono-window algorithm for retrieving land surface temperature from Landsat TM data and its application to the Israel–Egypt border region. *Int. J. Remote Sens.* 22, 3719–3746.
- SAGPyA, 2002. Primer inventario nacional de plantaciones forestales en macizo. SAGPyA Forestal 20.
- Santoni, C.S., Jobbágy, E.G., Contreras, S., 2010. Vadose transport of water and chloride in dry forests of central Argentina: the role of land use and soil texture. *Water Resour. Res.* 46, W10541.
- Scanlon, B.R., Reedy, R.C., Stonestrom, D.A., Prudic, D.E., Dennehy, K.F., 2005. Impact of land use and land cover change on groundwater recharge and quality in the southwestern US. *Glob. Change Biol.* 11, 1577–1593.
- Schaap, M.G., Leij, F.J., van Genuchten, M.T., 2001. Rosetta: a computer program for estimating soil hydraulic parameters with hierarchical pedotransfer functions. *J. Hydrol.* 251, 163–176.
- Schofield, N.J., 1992. Tree-planting for dryland salinity control in Australia. *Agrofor. Syst.* 20, 1–23.
- Šimunek, J., van Genuchten, M.T., Šejna, M., 2005. The HYDRUS-1D Software Package for Simulating the Movement of Water, Heat, and Multiple Solutes in Variably Saturated Media, Version 3.0, HYDRUS Software Series 1. Department of Environmental Sciences, University of California Riverside, Riverside, California, USA.
- Sizemskaya, M.L., Romanenkov, V.A., 1992. The evaluation of the desalinization rate of Solonchakous Solonchets in the Northern Caspian Region under agroforestry practice. *Pochvovedenie* 6, 83–91.
- Soriano, A., Leon, R.J.C., Sala, O.E., Lavado, R.S., Deregibus, V.A., Cahuepe, M., Scaglia, O.A., Velázquez, C.A., Lemcoff, J.H., 1991. Río de la Plata grasslands. In: Coupland, R.T. (Ed.), Natural Grasslands: Introduction and Western Hemisphere. Ecosystems of the World 8A. Elsevier, Amsterdam, pp. 367–407.
- Totis de Zeljkovich, L., Zeljkovich, J., Coca de Gonzalez, G., Blotta, L., Funston, L., Rivoltella, A., 1991. Balance del agua del doble cultivo trigo-soja y su relación con la productividad en la región de Pergamino [R. Argentina]. Informe técnico. EEA Pergamino, no. 257. INTA, Pergamino, p. 14.
- UMSEF, 2008. Monitoreo de la superficie de bosque nativo de Argentina. Secretaría de Ambiente y Desarrollo Sustentable, <http://www.ambiente.gov.ar/>.
- USDA, 1986. Urban Hydrology for Small Watersheds. TR55. United States Department of Agriculture, Washington, p. 164.

- van Genuchten, M.T., 1980. A closed-form equation for predicting the hydraulic conductivity of unsaturated soils. *Soil Sci. Soc. Am. J.* 44, 892–898.
- van Genuchten, M.T., 1987. A numerical model for water and solute movement in and below the root zone. In: Research Report No. 121. U.S. Salinity Laboratory, USDA, Riverside, California.
- Vervoort, R.W., Minasny, B., Cattle, S.R., 2006. The hydrology of Vertosols used for cotton production. II. Pedotransfer functions to predict hydraulic properties. *Aust. J. Soil Res.* 44, 479–486.
- Viglizzo, E.F., Frank, F.C., 2006. Ecological interactions, feedbacks, thresholds and collapses in the Argentine Pampas in response to climate and farming during the last century. *Quaternary Int.* 158, 122–126.
- Viglizzo, E.F., Jobbágy, E.G., Carreño, L.V., Frank, F.C., Aragón, R.M., De Oro, L., Salvador, V.S., 2009. The dynamics of cultivation and floods in arable lands of central Argentina. *Hydrol. Earth Syst. Sci.* 13, 491–502.
- Zhang, L., Dawes, W.R., Walker, G.R., 2001. Response of mean annual evapotranspiration to vegetation changes at catchment scale. *Water Resour. Res.* 37, 701–708.